International Journal of Applied Earth Observation and Geoinformation 18 (2012) 548–556

Contents lists available at SciVerse ScienceDirect

International Journal of Applied Earth Observation and Geoinformation

journal homepage: www.elsevier.com/locate/jag

A tool for rapid post-hurricane urban tree debris estimates using high resolution aerial imagery

Zoltan Szantoi[a,*], Sparkle Malone[b], Francisco Escobedo[c], Orlando Misas[d], Scot Smith[e], Bon Dewitt[f]

[a] School of Forest Resources & Conservation – Geomatics, 404A Reed Lab P.O. Box 110565, University of Florida, Gainesville, FL 32611, USA
[b] School of Forest Resources & Conservation, 136 Newins-Ziegler Hall, P.O. Box 110410, University of Florida, Gainesville, FL 32611-0410, USA
[c] School of Forest Resources & Conservation, 361 Newins-Ziegler Hall, P.O. Box 110410, University of Florida, Gainesville, FL 32611-0410, USA
[d] Department of Electrical and Computer Engineering, P.O. Box 116200, 216 Larsen Hall, University of Florida, Gainesville, FL 32611-6200, USA
[e] School of Forest Resources & Conservation – Geomatics, 301 Reed Lab, P.O. Box 110565, University of Florida, Gainesville, FL 32611-0565, USA
[f] School of Forest Resources & Conservation – Geomatics, 305 Reed Lab, P.O. Box 110565, University of Florida, Gainesville, FL 32611-0565, USA

ARTICLE INFO

Article history:
Received 11 January 2011
Accepted 14 October 2011

Keywords:
Hurricane debris assessment
Edge detection
Color filtering
Urban forest management

ABSTRACT

Coastal communities in the southeast United States have regularly experienced severe hurricane impacts. To better facilitate recovery efforts in these communities following natural disasters, state and federal agencies must respond quickly with information regarding the extent and severity of hurricane damage and the amount of tree debris volume. A tool was developed to detect downed trees and debris volume to better aid disaster response efforts and tree debris removal. The tool estimates downed tree debris volume in hurricane affected urban areas using a Leica Airborne Digital Sensor (ADS40) and very high resolution digital images. The tool employs a Sobel edge detection algorithm combined with spectral information based on color filtering using 15 different statistical combinations of spectral bands. The algorithm identified downed tree edges based on contrasts between tree stems, grass, and asphalt and color filtering was then used to establish threshold values. Colors outside these threshold values were replaced and excluded from the detection processes. Results were overlaid and an "edge line" was placed where lines or edges from longer consecutive segments and color values within the threshold were met. Where two lines were paired within a very short distance in the scene a polygon was drawn automatically and, in doing so, downed tree stems were detected. Tree stem diameter–volume bulking factors were used to estimate post-hurricane tree debris volumes. Images following Hurricane Ivan in 2005 and Hurricane Ike in 2008 were used to assess the error of the tool by comparing downed tree counts and subsequent debris volume estimates with post-hurricane photo-interpreted downed tree counts and actual field measured estimates of downed tree debris volume. The errors associated with the use of the tool and potential applications are also presented.

1. Introduction

In 2005, Hurricane Ivan in the state of Florida in the United States (U.S.) caused an estimated US$14 billion in damages (Lott and Ross, 2006), making it the third costliest hurricane on record at the time. Pensacola Florida's buildings and urban trees were severely damaged after the hurricane. Duryea et al. (2007) collected field data on post-hurricane tree damage 2 days after Hurricane Ivan and Escobedo et al. (2009) and Staudhammer et al. (2009) assessed urban tree debris using 2004–2005 hurricane season debris removal data. Staudhammer et al. (2011) assessed hurricane effects on urban forest structure and Thompson et al. (2011) spatially analyzed tree debris volumes, or the cubic meters of post-hurricane large downed branches and tree stems per 400 m^2 random plots, in Houston Texas, U.S. following Hurricane Ike. While these studies used field measured urban forest damage and recovery costs, field data collection is very expensive and time consuming and, is hampered by safety and access issues (COES, 2005). As a result, there is a need to support local governments with timely information on the extent and severity of damage to urban forests in a more rapid and efficient manner.

Remote sensing can be used to address this need by contributing to the development of rapid image recognition systems. Post-hurricane imagery and an image recognition tool could be used to identify downed trees and estimate tree debris volumes. Similar remote sensing based approaches have been developed for determining characteristics using object-based analyses of forest vegetation (Mallinis et al., 2008), estimating aboveground

* Corresponding author. Tel.: +1 352 392 0345; fax: +1 352 392 4957.
E-mail addresses: zszantoi@ufl.edu (Z. Szantoi), slm@ufl.edu (S. Malone), fescobed@ufl.edu (F. Escobedo), omisa001@ufl.edu (O. Misas), sesmith@ufl.edu (S. Smith), bon@ufl.edu (B. Dewitt).

0303-2434/$ – see front matter © 2011 Elsevier B.V. All rights reserved.
doi:10.1016/j.jag.2011.10.009

biomass (Okuda et al., 2004), differentiating spatial and spectral characteristics of tree crowns (Sugumaran et al., 2003), and for the identification of individual tree species (Key et al., 2001). For example, Barnes et al. (2007) developed an image-driven data mining approach with a sigma-tree structure, that tested IKONOS multispectral (2 m × 2 m RGB and NIR) and IKONOS-2 (1 m × 1 m) panchromatic images. Their approach resulted in 70% and 82% detection accuracy of trees and grass, respectively.

Other methods have also used Geographic Information System (GIS) to estimate large scale damage to forests. Pickens et al. (2002) used GIS to identify and digitize damaged forested areas that had 75–100% downed trees following Hurricane Fran in North Carolina in the U.S. However, their objective was pre-fire suppression planning rather than estimating post-storm downed tree debris volume. They also used ArcGIS Spatial Analyst with field data and an Inverse Distance Weighted method to interpolate damaged areas. After Hurricane Isabel in North Carolina, Shedd and Devine (2005) estimated downed woody debris using Feature Analyst (FA), an ArcGIS object oriented classifier. The authors used small scale (1:6000) digital aerial photos that were true color and color infrared and then employed: supervised and unsupervised classification techniques, leaf area index, and Normalized Difference Vegetation Index (NDVI) to identify downed woody debris. Since spectral responses did not quantify all areas with downed woody debris, they used the ArcGIS Feature Analyst and focused on spectral characteristics as well as spatial patterns. While the FA mapped areas of downed trees, it could not quantify the downed woody debris volumes.

Another set of studies focused on estimating above ground biomass using medium resolution satellite imagery and regression techniques. Magnusson and Fransson (2005) estimated stand level tree volumes by averaging their reflectance values using Landsat bands 1, 2, 4, 5 and 7 and a regression analysis. Lefsky et al. (2001) used 1 m spatial resolution data to predict biomass using a regression model (*R* square = 0.47). Escobedo et al. (2009) also used Landsat data as part of their assessment in estimating hurricane debris following the 2004–2005 Florida hurricane season. Spruce and McKellip (2006) attempted a hurricane damage assessment using IKONOS imagery and a maximum likelihood classification. However, they were not able to show individual downed trees and they did not attempt to quantify tree debris amounts.

Spectral information using edge and color filtering has proven useful for identifying tree crowns (Wang et al., 2004), as well as in identifying different man-made objects such as vehicles (Soille and Pesaresi, 2002; Leduc and Lavigne, 2007). Soille and Pesaresi (2002) tested image segmentation where an algorithm computed erosions/dilations with discrete line segments of arbitrary orientation and length. And in doing so, they were able to extract long thin objects (city buses) from a 1-m panchromatic IKONOS image. Leduc and Lavigne (2007) tested three assisted feature extraction tools (Genie Pro-Observera Inc., Chantilly, VA, USA, Feature Analyst-Overwatch Systems Ltd., Sterling, VA, USA, and eCognition-Definiens AG, Munich, Germany) to detect ships and vehicles from a very high resolution true color image (32 cm). Genie Pro and the Feature Analyst follow a three-step process: sample collection, training and extraction. Conversely, eCognition uses an object-oriented approach to detect objects and provided the best results by successfully detecting ships on open water with high accuracy (96.6%). However, accuracy values significantly decreased to around 76% and "false alarm" rates increased (from 35% to 45%) when vehicles were detected on a parking lot. Moreover, it took about 8 h to process a small scale image (500 m × 500 m).

To our knowledge, there have been few studies that have reliably estimated post-hurricane urban tree debris volumes using very high resolution digital sensor data. To address this lack of information, this study combined post-hurricane, very high resolution digital aerial imagery, image processing (mathematical morphology, edge detection, and color filtering), and a recognition tool that can be utilized to rapidly detect post-hurricane downed trees and subsequently estimate downed tree debris volume. The specific objectives of this study were to utilize and assess a tool that: (1) detected downed trees in an urban environment and (2) estimated the resulting tree debris volume using spectral characteristics and downed tree counts. Results from this tool and approach can be used to estimate urban forest debris volumes using high resolution aerial images, as well as field estimates (Thompson et al., 2011), and USDA Forest Service ground debris volume estimation tables (Personal Communication, Dudley Hartel USDA Forest Service, August, 2009; COES, 2005).

1.1. Data

Planar rectified imagery was obtained using a Leica ADS40 digital sensor for Pensacola, Florida for areas impacted by Hurricane Ivan (2004) and for Houston, Texas in areas that were impacted by Hurricane Ike (2008) (www.3001Inc.com). The ADS40 is a push-broom multi-spectral sensor (Leica Geosystems GIS & Mapping LLC, Heerbrugg, Switzerland) with a 12,000 pixel swath. The sensor collects data in the visible spectra (red–green–blue; RGB bands) and, images are taken simultaneously from a single viewing angle with airborne global positioning system and inertial measurement unit data were used for georeferencing the raw imagery. The scenes were acquired at a 27 cm ground sample distance resolution for the Hurricane Ivan imagery and 15 cm for the Hurricane Ike imagery. The flight height for the Hurricane Ivan image was 3000 m and 1500 m above ground for Hurricane Ike. The image data were collected 2 days after Hurricane Ivan (September 18, 2004) and 10 days after Hurricane Ike (September 23, 2008) by 3001INC Geospatial Company. Two images were used for debris volume estimation in Pensacola following Hurricane Ivan; Pensacola_1 (245 ha) and Pensacola_2 (182 ha) (Fig. 1). Following Hurricane Ike, a 0.033 ha subset and a 0.167 ha subset were centered on each field control plot for better debris volume estimation in Houston, Texas. The imagery (Fig. 1) was captured at a 12-bit radiometric resolution and converted to 8-bit radiometric resolution during post-processing. Additional post-hurricane tree debris volume field data were collected 6 weeks after Hurricane Ike (October 25, 2008) as part of two parallel studies (Staudhammer et al. (2011); Thompson et al., 2011). Field data used in this analysis included four randomly located 0.02-ha plots that were compared with the Hurricane Ike imagery for Houston, Texas. However, field measurements could not be taken immediately after the hurricane due to safety and access issues (Staudhammer et al. (2011); Thompson et al., 2011). No post-hurricane tree debris field data related to this study were collected following Hurricane Ivan.

2. Methods

The tree detection algorithm was developed using sample points collected from representative downed trees on the Leica ADS40 images. Selecting representative downed trees on the tested images had the advantage of identifying and establishing representative values and thresholds for edge and color filtering by examining the collected digital numbers (DNs). After the initial sample point data were collected, the downed tree detection process consisted of four stages. The first stage was edge detection; the second was color filtering based on collected pixel values, the third was the analysis of the filtered image using line detection comparisons and in the final stage, the polygon – or tree stem-detection was finalized and tree diameters calculated (Fig. 2). Once tree diameter was obtained, tree debris volumes were estimated using USDA Forest

Fig. 1. Images for Pensacola, Florida with selected neighborhoods used in the analysis. Images were taken two days following Hurricane Ivan (September 18, 2004). The upper and lower right windows are zoomed in areas depicting downed trees.

Service conversion factors for tree stem diameter–debris volume relationships.

The Tree Detection Tool programming was done in Microsoft Visual Studio 2005 in C# language and AForge.Net (www.aforgenet.com) was used for image processing applications. Rather than processing the data, AForge.Net actually analyzes the processed data and is an open-source framework for image processing, machine vision, and for developing genetic and neural network algorithms. Statistical analyses such as means and standard deviations were performed using JMP statistical software to determine the optimum values for the filtering techniques. After applying the filters, data were used to estimate the tree debris volume in the images.

Mathematical morphology transformations were based on erosion, dilation, opening, and closing operations (Serra, 1982). There are more advanced morphologic filters, however, they have the disadvantage of distorting image quality (Cheng and Venetsanopoulos, 2002). Since pixel counts were used to estimate tree diameter; any distortion would result in inaccurate measurements. To circumvent this, we used edge detection for our image processing. Edge detection, as defined in this study, is the measure of color constancy and changes from one color to the next. These changes are then modeled as a grayscale image where the intensity of the gray line represents the change from color to color. Thus, grayscale images form a more realistic interpretation of most “real” edges on the image (van de Weijer et al., 2007). Because images in urban areas

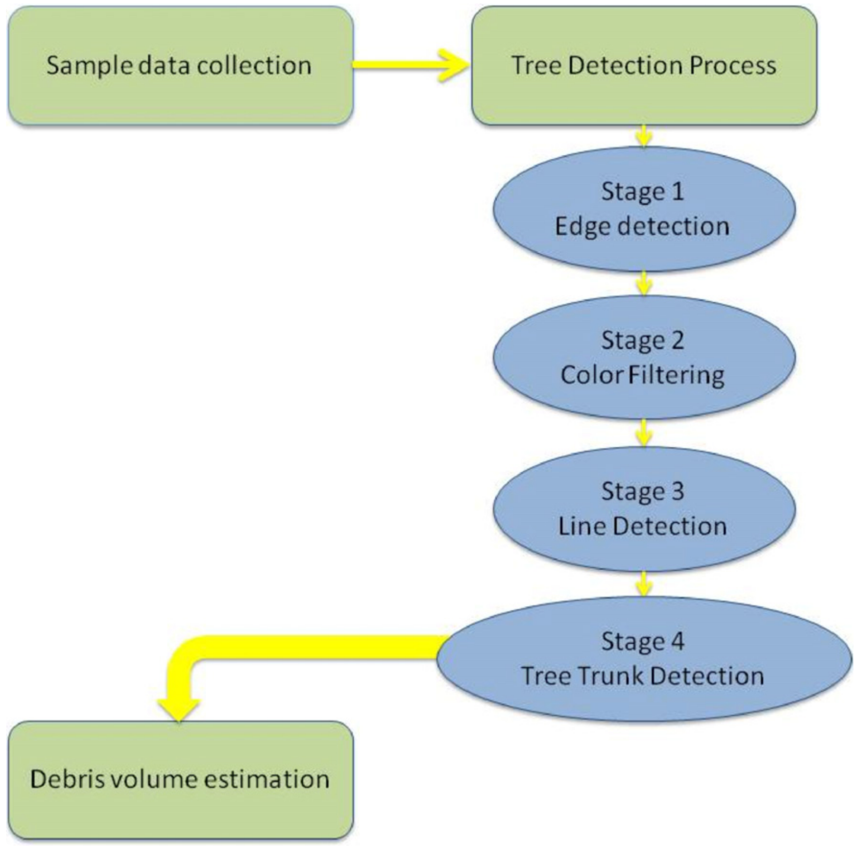

Fig. 2. The four stages in the downed tree detection tool workflow process.

can consist of roofs, streets, and standing trees that can complicate analyses, these features must be eliminated from the image. Finally, color filtering – in which a pre-determined color threshold based on manually verified color values, was selected for each band (less than 30) and all others were replaced by black – was used since tree stem colors are generally consistent. Although this method cannot distinguish between tree stems and roofs of the same color, the use of pre-determined boundary conditions can eliminate these errors.

Euclidean distance transformation has been found to improve the accuracy of color filtering techniques over a range of colors (Barni et al., 2000). So, it was used in our color filtering to create a sphere centered on pre-selected threshold values for the RGB bands and an effective radius, or range, of acceptable color values for the tree stems. A graphical representation of subspace V is shown in Fig. 3 where V_1, V_2 and V_3 represent the RGB channels. In the collected imagery most tree stems had color values ranging between 15 and 25 DN in each of the bands; by centering the sphere at (20, 20, 20) with a radius of 8 DNs, the colors were left with a relatively small amount of undesired values.

In doing so, each color is represented as a vector, then based on Euclidean geometry, the distance to a point (i.e. the center of the sphere) can be viewed as the square root of the sum of the distance squared in each axis (Barni et al., 2000) as illustrated by Eq. (1)

$$V(\vec{v}) = ||\vec{v}|| = \sqrt{\sum_{i=1}^{n} v_i^2} \quad (1)$$

where, $\vec{v}$ corresponds to the color of the pixel in question and v_i represents the difference between the center color value and the pixel

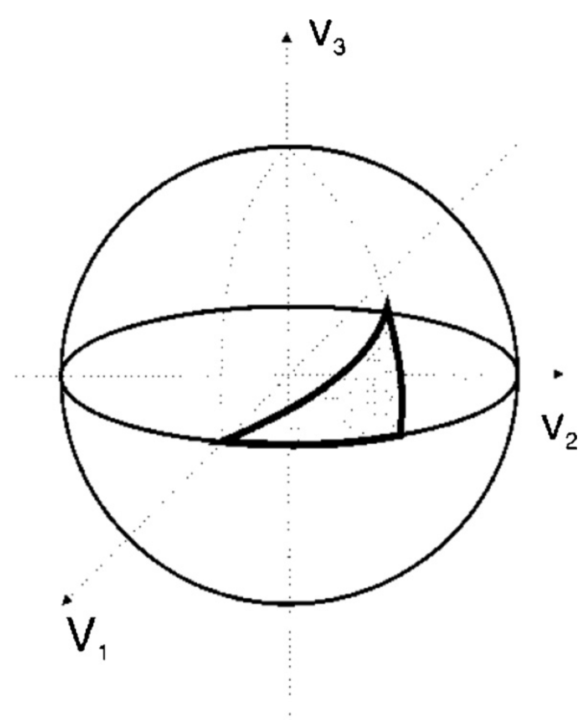

Fig. 3. Graphical representation of the subspace V, where V_1, V_2 and V_3 represent the red–green–blue (RGB) channels.
Modified from Barni et al. (2000).

color value for a specific channel. When applied to our RGB color filtering, it resulted in three bands ($n = 3$). A disadvantage of color filtering using Euclidean distance transformation is its long processing time and the amount of required memory since for an $n \times n$ color image where n is the number of rows and columns; the algorithm runs in $O(n^2)$ time and takes $O(n^2)$ space (Sudha et al., 1998). Once the angle between a downed tree and horizontal axes were detected, a rectangle was drawn over the image, and the angle used to delineate a whole tree stem including its crown. The resulting rectangles were progressively reduced until approximately 98–99% were a color other than black.

2.1. Algorithm development

The four stages in Fig. 2 were used for tree stem detection and subsequent tree debris volume estimates in our tool. Edge filtering (stage 1 in Fig. 2) utilized a Sobel edge detection method, where convolution kernels for y and x were calculated as shown in Eq. (2). These were then applied to obtain gradient estimates in the $y(G_y)$ and $x(G_x)$ directions, respectively, for each pixel in the image.

$$G_y = \begin{bmatrix} +1 & +2 & +1 \\ 0 & 0 & 0 \\ -1 & -2 & -1 \end{bmatrix} \quad \text{and} \quad G_x = \begin{bmatrix} +1 & 0 & -1 \\ +2 & 0 & -2 \\ +1 & 0 & -1 \end{bmatrix} \tag{2}$$

An estimate of the magnitude of the overall edge gradient (G) was calculated using Eq. (3). This method highlighted most of the details on the image; however, small and minor edges were also highlighted (Gonzalez, 2008).

$$G = \sqrt{G_y^2 + G_x^2} \tag{3}$$

The color filtering (stage 2 in Fig. 2) used a dynamic statistical model, where a dataset of acceptable points was collected by user-selected representative points (visual selection) from downed trees on the image. Because this method is dynamic and does not store the statistical values after they are used, the algorithm is more versatile and hence, less susceptible to common errors such as varying sun angles from local zenith or the different viewing angles from the sensor. The resulting data set is composed of maximum and minimum values for each sub-color in the RGB bands, hue, lightness, and saturation (HLS) bands and yellow, magenta, cyan (YMC) bands. In addition, the *differential* – or the degree of difference – between two bands was used as the basis for the algorithm since the strongest filter was the mean with twice the standard deviation (SD) for threshold values. Standard deviation is based on all the pixels in the training set (min–max) in a single channel. A count was then done for each channel and *difference* values were taken as RG_2 (1SD) and BG_2 and BR_2 (1.5SD) (Table 1). The algorithm considered 15 different statistical combinations of the RGB bands in determining color filtering.

The filtering stage also used the threshold values coupled with maximum and minimum values to filter every pixel in the image while replacing pixels outside the range with a black color. Color filtering was done using the original image but changes were continuously updated on the image that resulted from the edge detection. After the filtering was complete the assumption was made that every pixel in the image that was not black was a tree stem. In doing so, lines were drawn on longer consecutive segments of edges that remained after the color filtering. These lines were evaluated by their lengths; assuming that each line must be between 135 cm and 400 cm to be considered a downed tree stem. These numbers are based on empirical assumptions and personal communication with USDA Forest Service Personnel. The lines were estimated using a mean square error optimization since mean square error comprises both the variance and the squared bias (Hansson-Sandsten and Sandberg, 2010).

In stage 3 of Fig. 2, the algorithm then detected pairs of lines, which represented the edges of a downed tree stem based on the criteria that lines within a certain distance of each other (160 cm) were sufficient to characterize a biologically realistic tree stem. Finally in stage 4 (Fig. 2), the algorithm added each set of paired lines (i.e. tree trunks) to the list of trees if the distance between the lines was less than 160 cm.

Once paired lines were identified, the pairs were connected at the top and bottom to form a polygon. For each tree, the algorithm can draw several polygons due to differences in angles, lengths and width. These polygons represented the tree stem. For tree stems to be added to the "main tree list" they must have a maximum area less than 72,900 cm^2 (about 100 pixel with ground sampling distance of 27 cm) but greater than 10,000 cm^2 (based on empirical measurements) (Fig. 4). The "main tree list" was composed of downed trees recognized by the tool and was used to develop the volume estimates for a selected scene from the image. Downed tree stem diameters were calculated based on the distance (pixel resolution) between the paired lines of the polygons. Downed trees with multiple polygons and which did not meet the criteria required for the addition to the main tree list were added to a secondary list.

The final tree debris algorithm process consisted of using tree diameter–debris conversion factors used by USDA Forest Service Post-Hurricane Strike Teams to calculate downed tree debris volumes (Personal Communication, Dudley Hartel USDA Forest Service, August, 2009).

Table 1
Statistical combinations of the color filtering phrase.

Band	Percent considered for threshold values	Formula
Red (R), green (G), blue (B)	95.45%	From image
Hue (H), luminance (L), saturation (S)	95.45%	$\tan(H) = \frac{\sqrt{3(G-B)}}{2R-G-B}$ $L = \frac{M+m}{2}$ $S = 255 \times \frac{(M-m)}{(M+m)}, \quad \text{if} \quad L < 128$ Otherwise; $S = 255 \times \frac{M-m}{511-(M+m)}$
Yellow (Y), magenta (M), cyan (C)	95.45%	$Y = R + G$ $M = R + B$ $C = G + B$
Differential (RG, BG, BR)	95.45%	$RG_1 = (R - G)/(R + G)$ $BG_1 = (B - G)/(B + G)$ $BR_1 = (B - R)/(B + R)$
Difference (RG, BG, BR)	68.27% 86.64% 86.64%	$RG_2 = R - G$ $BG_2 = B - G$ $BR_2 = B - R$

M is maximum (R, G, B) and m is minimum (R, G, B).

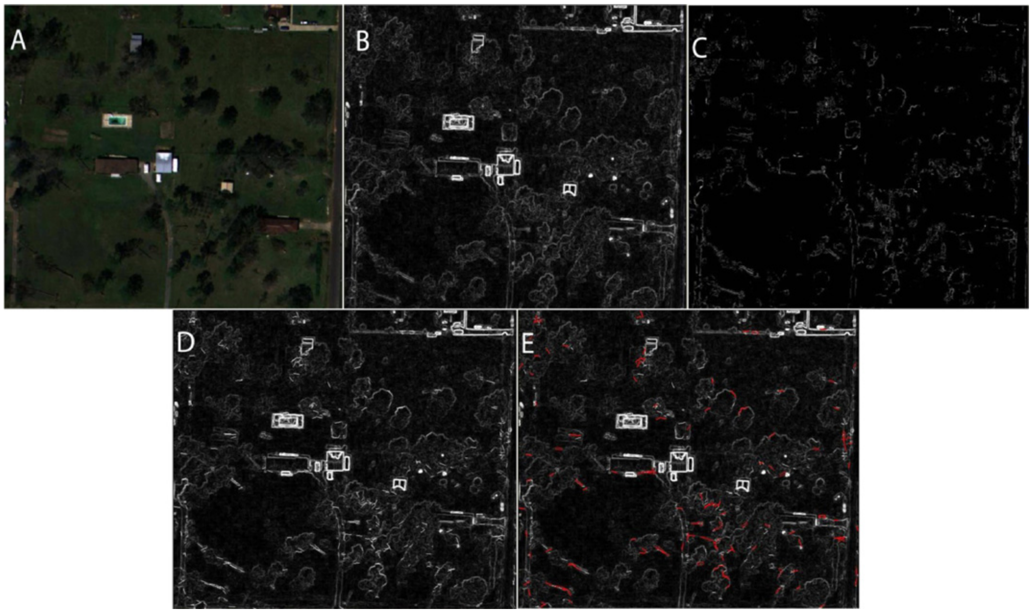

Fig. 4. The processing stages of the downed tree detection tool. (A) original image, (B) edge detection stage, (C) color filtering stage, (D) line detection/comparison stage, and (E) polygon tree detection/debris volume calculation stage.

Table 2
USDA Forest Service Center for Urban and Interface Forestry's ground debris conversion factor estimation table.

Tree stem diameter (cm)	Tree debris volume (m^3)
10	0.07
20	0.4
30	1.50
50	5.35
70	15.30
100	38.20
130	76.45
150	114.70

2.2. Debris volume estimation

Using the estimated diameters of all trees in our scenes, we calculated tree debris volume in cubic meters using the Debris Volume Estimation Table (Personal Communication, Dudley Hartel USDA Forest Service, August, 2009). This table contains conversion factors for calculating whole tree volume based on the average diameter of detected downed trees (Table 2) assuming that tree debris volume is approximately 50% wood and 50% air. Although these conversion factors are based on broad assumptions, resulting debris volumes quantify estimates that are regularly used for post-hurricane debris assessment activities (COES, 2005).

3. Error assessment

Error assessment was performed using two different sets of post-hurricane aerial imagery. The first assessment was used to determine the tool's ability to identify downed trees relative to the number of selected representative downed trees. The first set of imagery was taken 2 days after Hurricane Ivan's landfall on Pensacola, Florida (September 18, 2004). The approximate areas of the images were; Pensacola 1 – 245 ha (1860 × 1816 pixels) and Pensacola 2 – 182 ha (1347 × 1866 pixels) (see Fig. 1). To assess error, we first tallied the actual number of photo-interpreted downed trees using two sub-images (Fig. 1) clipped from the Pensacola 1 and 2 images. Ocular estimates of the number of fallen trees were made using ArcGIS software. The estimated number of photo-interpreted downed trees in the images was then compared to results obtained from the downed tree detection tool. Results from the downed tree detection tool, using 11 representative tree points, are shown in Fig. 5.

To determine the optimum number of points needed to obtain more reliable results based on our ocular photo-interpreted downed tree tallies, we used different numbers of representative downed trees (Table 3). For each number of representative trees, the tool was run 5 times and different trees were selected in each of the separate runs. Second, georeferenced field measurements of post-Hurricane Ike downed trees and debris volume following

Table 3
Estimated number of post-Hurricane Ivan downed trees using the downed tree detection tool for Pensacola, Florida using 2 different size images.

Image (pixel numbers)	Number of representative downed trees used for sample data collection (# points)				
Pensacola_1	6	11	17	23	45
Average number of trees found using 5 executions of the tool (5 tool runs)	479.8	648.6	699	686.8	691
Ocular estimate of downed trees	622	622	622	622	622
Error[a]	−142.2	26.6	77	64.8	69
Standard Error	102.6	26.3	23.2	16.9	17.9
Pensacola_2	6	11	23	34	45
Average number of trees found using 5 executions of the tool (5 tool runs)	498.4	660.4	687.6	679.8	638.6
Ocular estimate of downed trees	610	610	610	610	610
Error[a]	−111.6	50.4	77.6	69.8	28.6
Standard Error	64.2	8.3	13.3	17.1	8.5

[a] Error was calculated based on the difference between the manually counted downed trees and the trees detected by the tool.

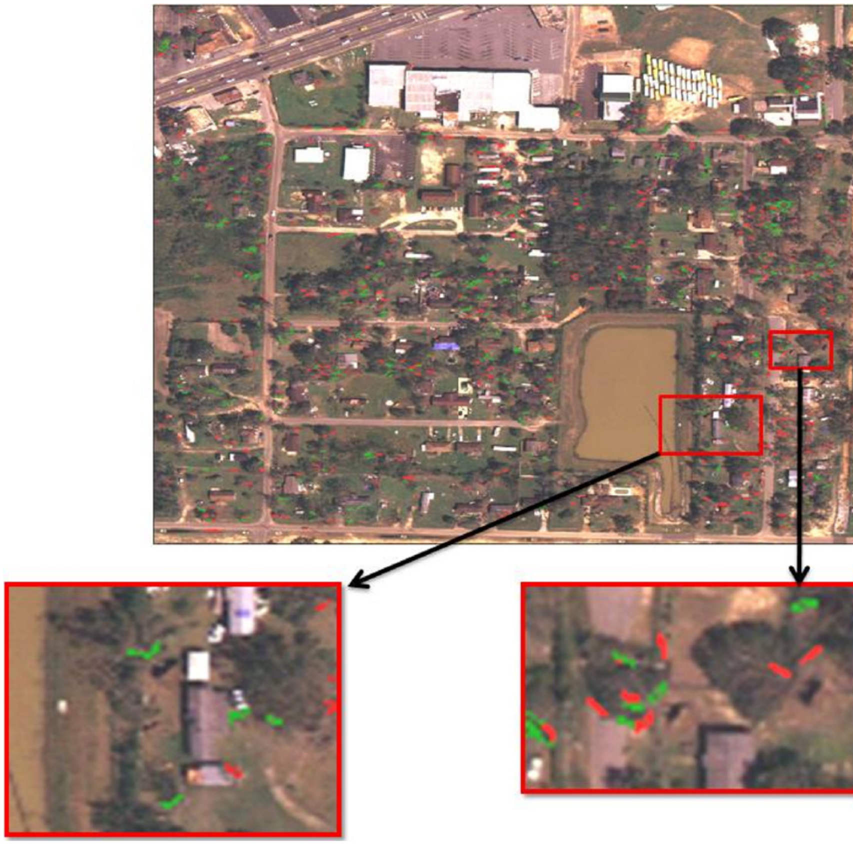

Fig. 5. Downed tree detection tool results for Pensacola, Florida. Red colored shapes indicate detected downed trees and green colored shapes are possible downed trees. (For interpretation of the references to color in figure legend, the reader is referred to the web version of the article.)

methods outlined in Thompson et al. (2011) were also used to determine the accuracy of the tool's volume estimates.

Analyses of variance and multiple *t*-tests determined that there were no significant differences between the numbers of sample trees selected and the tool using the Pensacola–1 image (Table 4). For the Pensacola_2 image there were, significant differences (alpha < 0.05) only when selecting 11 trees, 23 trees, and 45 trees. The optimum tree selection was between 11 and 45 trees and selecting 45 trees produced the smallest error yet selecting 11 trees produces the smallest deviation from the mean value. However, based on results from both images, we consider that selecting 11 trees per scene was optimum since this number of representative downed tree points yielded the most consistent estimates

Table 4
T-tests for significant difference between the number of sampled post-hurricane, representative downed tree selections using the downed tree detection tool for Pensacola, Florida.*

Pensacola_1				
Number of trees selected	11	17	23	45
6	n.s.	n.s.	n.s.	n.s.
11	n.s.	n.s.	n.s.	n.s.
17	n.s.	n.s.	n.s.	n.s.
23	n.s.	n.s.	n.s.	n.s.
Pensacola_2				
Number of trees selected	11	23	34	45
6	n.s.	n.s.	n.s.	n.s.
11	n.s.	0.05**	n.s.	0.05**
23	n.s.	n.s.	n.s.	0.05**
34	n.s.	n.s.	n.s.	n.s.

* n.s. denotes no significant difference at alpha >0.05.
** Significant difference at 95% significance level.

(Table 3). The collection of additional sample trees would likely introduce greater error due to the lack of available representative trees necessary to characterize downed trees. Unfortunately, ground debris volume data for the Pensacola study area were not available.

Since the sample data collection process for selecting representative downed trees is key to this study's algorithm, aside from determining the optimum number of tree points, we also assessed the optimum size of the image for sample data collection. We used information from Hurricane Ike and two different scene sizes – 0.033 ha and 0.167 ha – to determine the optimal size for the sample data collection of representative downed trees (Fig. 6). Images were centered on field debris measurements plots described in Thompson et al. (2011) and Staudhammer et al. (2011). Specifically, post-hurricane tree debris data used in this analysis was collected at four random previously measured 0.02 ha (0.6 acre) field plots within urban Houston, Texas 6 weeks following Hurricane Ike (Thompson et al., 2011). Each plot was then used to assess the estimates obtained for the tool on separate 0.167 ha (5 acre) and 0.033 ha (1 acre) images. To test the accuracy of the tool, ocular estimates of downed trees were collected for these images and tool results were compared to field data.

The number of downed trees on all images was manually tallied using photo-interpretation. The trees debris volume on 0.02 ha ground control plots were converted to tree debris volume per ha and, these numbers were used as reference values for the error assessment (Table 5).

Results indicate that 0.033 ha sized plots were consistently underestimating downed trees (Table 5). This is may be the result of the lack of ideal tree selection for image processing when using a smaller plot size. Interestingly, even though tree numbers were

Fig. 6. The 0.033 ha (upper row) and 0.167 (lower row) ha scenes following Hurricane Ike in Houston, Texas that were used for selecting image size for sample data collection of representative downed trees.

under estimated, volume was being over estimated (Table 5). Results also show that 0.167 ha plots overestimated the number of downed trees (Table 5). When evaluating the errors of the tool, there appears to be error introduced by the presence of sidewalks and roofs. Tree debris volume estimates for these plots were also influenced by image acquisition dates and ground data issues outlined in Thompson et al. (2011) as well as scaling issues associated with using 0.02 ha plots to represent larger landscapes. However, smaller image sizes did yield greater variation and error in downed tree selections. This might be largely due to the larger introduction of error from the increased complexity in the scene with increasing scales. Most plots were over estimating the amount of tree debris volume in the images and the differences might be due to the time lag between image collection and ground data collection. According to Thompson et al. (2011) and Staudhammer et al. (2011), the ground data was collected several days after the hurricane and tree debris removal was most likely to have occurred during this time period. Thus, Table 5 should be used for informational purposes only and not for actual comparisons between the ground-collected data and the tool results for debris volume.

4. Limitations

The tool developed in this study was limited by the cross-sectional nature of our datasets and our inability to distinguish downed trees from a number of other urban features such as fences around urban structures and shadows caused by buildings as these affected the resulting error in our assessment. Additionally, shadows from standing trees can also be detected as a downed tree due to their shape and color. Bare soil on dirt roads and open fields, as well as rooftops and sidewalks also resembled the color variations in tree stem bark and as a result were another possible source of error. Finally, a limitation of this method is its inability to measure downed branches from standing trees and small diameter trees as these can also contribute to total tree debris amounts.

Further research is warranted in using rapidly acquired post-hurricane debris data with immediate, post-hurricane georeferenced high resolution imagery. Additionally, high sampling density, small footprint Light Detection and Ranging (LiDAR) data could be fused with segmented, high resolution aerial photography to measure downed tree debris volume in three dimensions following hurricane landfall. Ancillary spatial data such as parcel

Table 5
Estimated number of downed trees and debris volume in cubic meters using 0.033 ha and 0.167 ha plots for Houston Texas following Hurricane Ike.

	Average fallen trees (SD)	Average debris volume (SD)	Observed fallen trees (count)	Observed volume
Plots (0.033 ha)				
704	175.4 (40.27)	11401.8(5519)	111	31.6
843	48.8 (41.36)	2470.2(2181)	5	57.3
1130	67 (47.57)	4013.9(3552)	9	1149.4
1239	62.8 (57.55)	4517.7(3768)	55	409.5
Plots (0.167 ha)				
704	900.8 (490.31)	71016.4(55,007)	728	157.9
843	695.6 (95.34)	54164.8(35,652)	82	286.7
1130	447.6 (360.22)	12626.6(10,302)	138	5746.8
1239	748.4 (355.9)	32690.8(15,066)	327	2047.5

SD – standard deviation.

tract characteristics and digital elevation model could also be used identify and remove buildings and fences from an image prior to running our tool, thus improving our error estimates.

5. Conclusion

This study developed a tool that was rapid and relatively reliable for estimating post–hurricane downed trees and subsequent debris volume when compared to estimates obtained using photo-interpretation and field measured data volume estimates. The tool could potentially be used by emergency management agencies and urban forest managers to rapidly and easily estimate downed tree debris volume after natural disasters (COES, 2005). Actual post-hurricane debris assessments, in the same area, that accounted for downed trees took several hours and had considerable logistical and safety issues (Duryea et al., 2007; Escobedo et al., 2009; Staudhammer et al., 2009, 2011; Thompson et al., 2011). The tool resulted in a reasonable estimate of the number of downed trees and tree debris volume following hurricane events. The program converged quickly using an Inter Centrino Duo 2.00 GHz processor and 2 GB of RAM using the ADS40 images (less than 1 min). The authors believe that the 12 in. spatial resolution is sufficient to produce accurate tree diameter values. If the cost of acquiring the aerial imagery's cost is not prohibitive, the methodology could have important and timely emergency management and natural disaster response applications.

Acknowledgements

The authors give special thanks to Dr. Clint Slatton, who provided valuable assistance to this project prior to his untimely death on March, 2010. This research was funded by the USDA Forest Service, Centers for Urban and Interface Forestry and the Florida Division of Forestry. The authors would like to thank Shravan Pyata, and Dudley R. Hartel for support and help. Finally, the authors would like to thank the editor and anonymous reviewer for their valuable comments and recommendations that have improved the quality of our manuscript.

References

Barnes, C.F., Fritz, H., Yoo, J., 2007. Hurricane disaster assessments with image-driven data mining in high-resolution satellite imagery. IEEE Transactions on Geoscience and Remote Sensing 45, 1631–1640.

Barni, M., Buti, F., Bartolini, F., Cappellini, V., 2000. A quasi-Euclidean norm to speed up vector median filtering. IEEE Transactions on Image Processing 9, 1704–1709.

Cheng, F., Venetsanopoulos, A.N., 2002. An adaptive morphological filter for image processing. IEEE Transactions on Image Processing 1, 533–539.

COES (California Office of Emergency Services), 2005. Disaster Debris Management Training Manual. Governor's Office of Emergency Services, State of California, p. 118. http://www.calema.ca.gov/Recovery/Documents/Chapter4.pdf (accessed 08.15.2011).

Duryea, M.L., Kampf, E., Littell, R.C., Rodríguez-Pedraza, C.D., 2007. Hurricanes and the urban forest: II effects on tropical and subtropical tree species. Arboriculture & Urban Forestry 33, 98–112.

Escobedo, F., Luley, C.J., Bond, J., Staudhammer, C., Bartel, C., 2009. Hurricane debris and damage assessment for Florida urban forests. Arboriculture & Urban Forestry 35, 53–59.

Gonzalez, R., 2008. Digital Image Processing, 3rd ed. Prentice Hall, Upper Saddle River, NJ.

Hansson-Sandsten, M., Sandberg, J., 2010. Optimization of weighting factors for multiple window spectrogram of event related potentials. EURASIP Journal on Advances in Signal Processing 2010, 10.

Key, T., Warner, T.A., McGraw, J.B., Fajvan, M.A., 2001. A comparison of multispectral and multitemporal information in high spatial resolution imagery for classification of individual tree species in a temperate hardwood forest. Remote Sensing of Environment 75, 100–112.

Leduc, F., Lavigne, D.A., 2007. Comparing several AFE tools in the context of ships and vehicles detection based on RGB and EO data. In: 10th International Conference on Information Fusion, 9–12 July, pp. 1–7.

Lefsky, M.A., Cohen, W.B., Spies, T.A., 2001. An evaluation of alternate remote sensing products for forest inventory, monitoring, and mapping of Douglas-fir forests in western Oregon. Canadian Journal of Forest Research 31, 78–87.

Lott, N., Ross, T., 2006. Tracking and Evaluating U.S. Billion Dollar Weather Disasters, 1980–2005. National Climatic Data Center.

Magnusson, M., Fransson, J., 2005. Estimation of forest stem volume using multispectral optical satellite and tree height data in combination. Scandinavian Journal of Forest Research 20, 431–440.

Mallinis, G., Koutsias, N., Tsakiri-Strati, M., Karteris, M., 2008. Object-based classification using Quickbird imagery for delineating forest vegetation polygons in a Mediterranean test site. ISPRS Journal of Photogrammetry and Remote Sensing 63, 237–250.

Okuda, T., Suzuki, M., Numata, S., Yoshida, K., Nishimura, S., Adachi, N., Niiyama, K., Manokaran, N., Hashim, M., 2004. Estimation of aboveground biomass in logged and primary lowland rainforests using 3-D photogrammetric analysis. Forest Ecology and Management 203, 63–75.

Pickens, L.M., Cheshire, H.M., Devine, H.A., 2002. Use of geographic information systems and photogrammetric techniques to improve the NC division of forest resources pre-suppression fire planning and forest management. In: Geoscience and Remote Sensing Symposium, 2000. Proceedings. IGARSS 2000. IEEE 2000 International, pp. 2712–2714.

Serra, J., 1982. Image Analysis and Mathematical Morphology. Academic Press, London, New York.

Shedd, J., Devine, H., 2005. Updating fuel fire loads and vegetation datasets after a natural disaster. In: EastFire Conference, Fairfax, VA, March.

Soille, P., Pesaresi, M., 2002. Advances in mathematical morphology applied to geoscience and remote sensing. IEEE Transactions on Geoscience and Remote Sensing 40, 2042–2055.

Spruce, J., McKellip, R., 2006. Assessing hurricane Katrina damage to the Mississippi Gulf coast using IKONOS imagery. In: JACIE Civil Commercial Imagery Evaluation Workshop, Laurel, MA, March.

Staudhammer, C., Escobedo, F., Luley, C., Bond, J., 2009. Patterns of urban tree debris from the 2004 and 2005 Florida hurricane season: A technical note. Southern Journal of Applied Forestry 33, 193–196.

Staudhammer, C., Escobedo, F., Lawrence, A., Duryea, M., Merritt, M., Smith, P., 2011. Rapid assessment of change and hurricane impacts to Houston's urban forest structure. Arboriculture and Urban Forestry 37, 60–66.

Sudha, N., Nandi, S., Bora, P., Sridharan, K., 1998. Efficient computation of Euclidean distance transform for applications in image processing. In: TENCON 98. 1998 IEEE Region 10 International Conference on Global Connectivity in Energy, Computer, Communication and Control. Presented at the TENCON 98. 1998 IEEE Region 10 International Conference on Global Connectivity in Energy, Computer, Communication and Control, vol. 1, pp. 49–52.

Sugumaran, R., Pavuluri, M., Zerr, D., 2003. The use of high-resolution imagery for identification of urban climax forest species using traditional and rule-based classification approach. IEEE Transactions on Geoscience and Remote Sensing 41, 1933–1939.

Thompson, B., Escobedo, F., Staudhammer, C., Matyas, C., Youliang, Q., 2011. Modeling hurricane-caused urban forest debris across in Houston Texas. Landscape and Urban Planning 101, 286–297.

van de Weijer, J., Gevers, T., Gijsenij, A., 2007. Edge-based color constancy. IEEE Transactions on Image Processing 16, 2207–2214.

Wang, L., Gong, P., Biging, G.S., 2004. Individual tree-crown delineation and treetop detection in high-spatial-resolution aerial imagery. Photogrammetric Engineering & Remote Sensing 70, 351–357.